Liquid Crystals

Publication details, including instructions for authors and subscription information:
http://www.informaworld.com/smpp/title~content=t713926090

Freeze-fracture electron microscopy of thermotropic cubic and columnar mesophases

Bertrand Donnio; Duncan W. Bruce

To cite this Article Donnio, Bertrand and Bruce, Duncan W.(1997) 'Freeze-fracture electron microscopy of thermotropic cubic and columnar mesophases', Liquid Crystals, 23: 1, 147 — 153

To link to this Article: DOI: 10.1080/026782997208758

URL: http://dx.doi.org/10.1080/026782997208758

LIQUID CRYSTALS, 1997, VOL. 23, NO. 1, 147–153

Freeze-fracture electron microscopy of thermotropic cubic and columnar mesophases

by BERTRAND DONNIO†, DUNCAN W. BRUCE*
Department of Chemistry, University of Exeter, Stocker Road, Exeter EX4 4QD, U.K.

HERVÉ DELACROIX* and THADDÉE GULIK-KRZYWICKI*
Centre de Génétique Moléculaire, CNRS, 91198 Gif-sur-Yvette Cedex, France

(*Received 24 January 1997; accepted 18 March 1997*)

Freeze-fracture electron microscopy has been applied to study thermotropic columnar and cubic phases of a polycatenar liquid crystal of silver(I). The columnar phases displayed hexagonal type II characteristic fracture planes. The cubic phases showed a fracture behaviour highly characteristic of the *Ia*3*d* type II (Q^{230}II) cubic space group, namely the high frequency of well ordered domains perpendicular to the [2 1 1] crystallographic axis and, much less frequently, the fragmented aspect of domains perpendicular to the [1 1 0] crystallographic axis. For both types of domain, the observed 2-D lattice parameters were in excellent agreement with the ideal values expected for the Q^{230} cubic space group.

1. Introduction

Cubic phases have long been known in the field of amphiphilic liquid crystals (surfactants [1] and lipids [2]) and plastic crystals [3], and have been studied extensively. Their name derives from X-ray diffraction studies, in which the Bragg reflections were indexed in cubic space groups. They show long range, three dimensional order, similar to that of classical crystals, but the presence of diffuse reflections in the wide angle region suggests a liquid-like, disordered state of the hydrocarbons chains. These phases appear transparent and optically isotropic in the polarizing microscope, owing to their cubic symmetry, occasionally making their identification troublesome.

In lyotropic systems, two types of cubic phase can be distinguished: the micellar (the organization within the mesophase consists of a three dimensional periodicity of the whole structure which is thought to be a cubic close-packed array of discrete, ovoid, micellar aggregates), and the bicontinuous (consisting of a single continuous bilayer which divides the space into two interwoven labyrinths), and they are located in different parts of the binary phase diagram according to their mean interfacial curvature [4]. In order to describe the three dimensional structure of the bicontinuous cubic phases, two models are used: the two three dimensional rod-networks or interlinking rods model proposed by Luzzati and Spegt [5], and the Infinite Periodic Minimal Surface (IPMS) model [6]. In lyotropic systems, the former description is more applicable to the bicontinuous cubic structures of type I (made of paraffinic rods merged in water) while the latter is more appropriate to describe the bicontinuous cubic structures of type II (water channels embedded in a 3-D complex bilayer). Indeed, in the case of those type II structures, the most paraffinic region (CH_3/CH_3 interface) happens to coincide with the Schwarz P–Schwarz D and the Gyroïd of Schoën surfaces being associated with the space groups, *Im*3*m*, *Pn*3*m* and *Ia*3*d*, respectively. Both descriptions provide a better understanding of the phase transitions (such as hexagonal/cubic or lamellar/cubic transitions) and the suggestion of possible intermediates, the mathematical passage from one topology to another being relatively simple [7]. The transformation from one structure to another (and thus the transformation of the topology) is closely related to the existence of epitaxial relationships between mesophases, and can be analysed experimentally.

Cubic phases have also been observed in conventional calamitic liquid crystal materials [8] but still remain rather rare, and thus their structures are not very well understood. Reports have also shown that cubic phases could be induced in binary mixtures [8 (*f*), 9].

We have reported the occurrence of cubic mesophases

---

†Present address: Institut de Chimie, 51 Avenue de Bellevaux, Université de Neuchâtel, Neuchâtel CH-2000, Switzerland.

*Author for correspondence.

in some silver(I) complexes of stilbazoles, their structure being shown in the figure below (figure 1: $m=12$, 14; $Y=Z=\mathrm{H}$, or $Z=\mathrm{F}$, $Y=\mathrm{H}$ or $Z=\mathrm{H}$, $Y=\mathrm{OC}_n\mathrm{H}_{2n+1}$).

The complexes with a dodecylsulphate anion [10] (figure 1: $m=12$, $Y=Z=\mathrm{H}$) were found to exhibit a cubic phase when the alkoxy chain length was hexyloxy or longer, the phase occurring between a SmC and a SmA phase. However, for the octylsulphate [11] and decylsulphate [12] derivatives (figure 1: $m=8$ and 10, $Y=Z=\mathrm{H}$), the cubic phase was not present and the complexes showed a more typical mesomorphism (N, SmA and SmC). The cubic phase reappeared for the tetradecylsulphate [13] derivatives (figure 1: $m=14$, $Y=Z=\mathrm{H}$). Interestingly, the cubic phase was also found in a few derivatives of the 4′-alkoxy-2′-fluoro-4-stilbazole silver(I) dodecylsulphate complexes [14] (figure 1: $m=12$, $Y=\mathrm{H}$, $Z=\mathrm{F}$), but not in its structural isomer (figure 1: $m=12$, $Y=\mathrm{F}$, $Z=\mathrm{H}$). In the 2-fluoro materials, the cubic phase appeared below the isotropic liquid and, in one case, below the nematic phase.

In a recent part of our studies on these silver systems, we described an X-ray determination of a cubic monodomain [15] obtained in some derivatives of the fluorinated and non-fluorinated silver dodecylsulphate systems. These monodomains were easily indexed in the *Ia*3*d* cubic space group, similarly to some lyotropic and other thermotropic materials. We have also reported the occurrence of the cubic phase in another series of silver complexes, in which the ligand possessed two alkoxy chains ($Z=\mathrm{H}$, $Y=\mathrm{OC}_n\mathrm{H}_{2n+1}$) [16]. In this system, the cubic phase appeared either between the crystalline and isotropic phases, or between the crystalline and columnar hexagonal phases.

In common with their lyotropic counterparts, thermotropic cubic phases show a very well-developed, long range, three dimensional order, and are also highly orientationally disordered as X-ray diagrams show a diffuse reflection at *c.* 4·5 Å, corresponding to the liquid-like state of the hydrocarbon chains. For the description of these structures, models similar to those used for the bicontinuous lyotropic cubic phases can be used too, that is the interlocked 3-D rod networks [17] and the IPMS models. There have so far been three different cubic space groups which have been identified for the cubic phases in thermotropic liquid crystals (*Ia*3*d*, *Im*3*m* and *Pm*3/*Pm*3*m*). However, the molecular organization within thermotropic mesophases is not so well understood as is the case in lyotropic systems.

Freeze-fracture electron microscopy (FFEM) has been widely used and successfully applied to the study of lyotropic liquid crystals and, in particular, to the characterization (structure and molecular organization) of the mesophases formed by the lipid–water systems. FFEM, combined with low temperature X-ray diffraction, is a powerful technique used to determine the structures of two and especially three dimensionally ordered mesophases. Indeed, the analysis of images of properly frozen samples displaying order in one or two dimensions were shown to be in excellent agreement with the structures determined by X-ray diffraction [18]. In particular, this technique allows a clear distinction between the two types of cubic structures that are the micellar and bicontinuous phases [19], which is not trivial by the use of X-ray scattering alone. FFEM has also been used to study blue phases [20] and $\mathrm{TGB_A}$ phases [21] in thermotropic systems.

Nevertheless, a problem that remains is that the intrinsic resolution of the micrographs tends to be rather low, leading to problems of interpretation for complex, three dimensional, liquid crystalline structures such as cubic phases. However, the quality of the images can be considerably enhanced using image filtering techniques based on correlation averaging, allowing a quantitative comparison of the electron microscopy structure to be made with that derived from X-ray diffraction experiments [22, 23]. Moreover, information that is not available from the X-ray powder patterns, such as the presence of rotation axes and mirror planes in the unit cell, can be directly revealed, helping to narrow down the range of possible space groups. These methods have been applied successfully both to type I and type II bicontinuous and micellar cubic phases [22, 23].

One of the main conclusions that can be drawn from that previous work is that for a given space group, the cubic phase displays different, highly characteristic, fracture behaviour, namely, the frequency, appearances and two dimensional lattice type and dimensions of different fracture planes. This conclusion suggests that

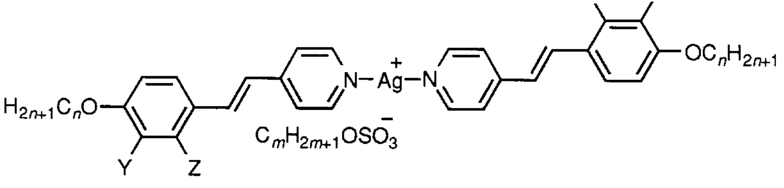

Y, Z = H, F or $\mathrm{OC}_n\mathrm{H}_{2n+1}$

Figure 1. General structure of the silver(I) dodecylsulphate complexes of stilbazoles exhibiting the cubic phase.

freeze-fracture electron microscopy, followed by appropriate image analysis, may be used for the determination of the type of lattices and the presence of different symmetry elements, helping the determination of the space group of different cubic phases.

In this communication, we report the study by freeze-fracture electron microscopy of the columnar and of the three-dimensionally ordered cubic phase present in some thermotropic silver complexes. For the purposes of these experiments, four samples were used. First we chose bis(4′-undecyloxy-4-stilbazole) silver(I) dodecylsulphate (figure 1: $m=12$, $n=11$, $Y=Z=\mathrm{H}$), since previously [15], we had shown by X-ray methods that two related complexes (with $n=9$ and 12) had a cubic phase with $Ia3d$ symmetry. It was therefore reasonable to assume that the cubic phase of the homologue with $n=11$ would have the same space group. Secondly, we chose three derivatives of the bis(3′,4′-dialkoxy-4-stilbazole) silver(I) dodecylsulphate (figure 1: $m=12$, $Z=\mathrm{H}$, $Y=\mathrm{OC}_n\mathrm{H}_{2n+1}$ with $n=5$, 6 and 11) complex series. These complexes showed cubic and columnar mesophases, and while we had been able to identify the columnar mesophase as having hexagonal symmetry, we did not know the symmetry of the cubic phase. The thermal behaviour of the four chosen materials is collected in the table.

2. Experimental

2.1. *Freeze-fracture electron microscopy*

For the present experiments, a few milligrams of the sample (powder) were placed on a thin copper holder maintained at a temperature corresponding to the presence of a phase to be studied. The sample was then rapidly quenched in liquid propane. The frozen sample was fractured at -125°C, in a high vacuum ($\approx 10^{-7}$ Torr), with the liquid-nitrogen-colled knife in a Balzers 301 freeze-etching unit. The replication was achieved by using unidirectional shadowing, at an angle of 35°C, with platinum–carbon, 1 to 1·5 nm of mean metal deposit. The replicas were washed with organic solvents and distilled water, and were observed in a Philips 301 electron microscope.

2.2. *Image selection and processing*

The whole procedure has been extensively described elsewhere [22] and needs only to be summarized here. Briefly, the micrographs are inspected in the search for ordered domains; the images of these domains are optically filtered, the dimensions of the 2-D lattices determined and their relative frequency assessed. The crystallographic orientation of each domain is then determined. A few well ordered domains were singled out, corresponding to the different previously observed orientations. Stereo views are used to select the domains whose fracture plane is virtually parallel to the plane of the image; further processing is used to improve the signal-to-noise ratio. A few selected images are digitized, the subdomains are identified and the cell parameters computed from their Fourier transform. Each subdomain is then Fourier-filtered using those cell parameters. Finally an area is selected and analysed using a cross-correlation averaging procedure [24]. The relationships between the different sub-domains are analysed by cross-correlating the domain with the averaged motif of one subdomain or by carefully Fourier filtering the whole domain. It must be stressed that no externally imposed symmetry operation is involved in the entire process.

3. Results and discussion

Freeze-fracture electron micrographs of the columnar phases of $[\mathrm{Ag\{St(6\text{-}3,4)\}_2}][\mathrm{DOS}]$ and $[\mathrm{Ag\{St(11\text{-}3,4)\}_2}][\mathrm{DOS}]$ (DOS = dodecylsulphate = $\mathrm{C_{12}H_{25}OSO_3}$) displayed characteristic features of the hexagonal phase of type II ($\mathrm{H_{II}}$), that is periodic parallel striations, the separation of which corresponds to the distance between hexagonally packed cylinders [18] (figure 2).

Freeze-fracture replicas of the cubic phase showed a rather complex fracture behaviour. In many places, as expected, the replica displayed regularly ordered fracture surfaces which, according to their optical diffraction patterns and to the dimensions of their two dimensional lattices, could be sorted into two classes of domains characteristic of the body-centred, $Ia3d$ cubic phase (Q^{230}) [22, 25]. One class corresponded to fracture domains that are perpendicular to the [2 1 1] crystallographic direction of this space group, the other to fracture domains perpendicular to the [1 1 0] crystallographic direction. The [2 1 1] domains are the most frequently observed and are usually fairly extended, while the [1 1 0] domains are only sparingly observed

Table Thermal behaviour of the compounds studied.

n	m	Y	Z	Mesomorphism (T/°C)
11	12	H	H	Cr 116 SmC 135 Cub 156 SmA 180 I
5	12	$\mathrm{OC_5H_{11}}$	H	Cr 76 Cub 116 I
6	12	$\mathrm{OC_6H_{13}}$	H	Cr 61 Cub 118 $\mathrm{Col_h}$ 153 I
11	12	$\mathrm{OC_{11}H_{23}}$	H	Cr 69 Cr′ 82 $\mathrm{Col_h}$ 176 I

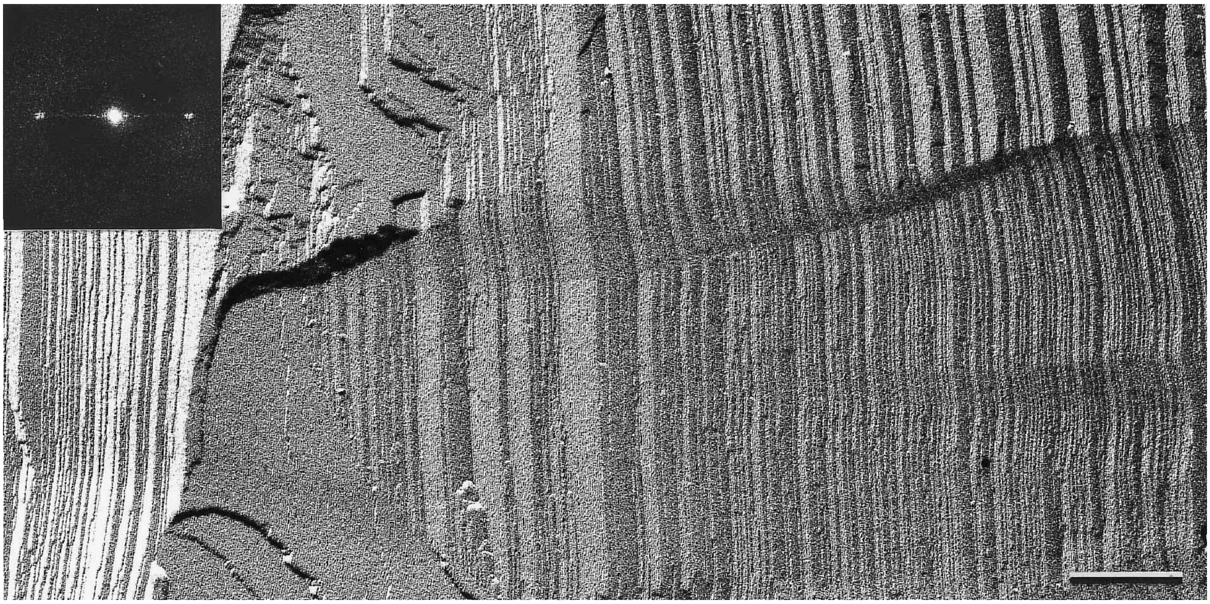

Figure 2. Freeze-fracture electron micrograph of the columnar phase for [AgSt(11-3,4)$_2$][DOS]. The optical diffraction of its lower left part is shown on the upper left corner; the bar represents 200 nm.

and their surfaces looked like a mosaic of tiny sub-domains.

The [2 1 1] fracture domains (figure 3) were almost flat and made of a succession of large successive cleavage planes, each of these sub-domains displaying the same parallel striations. The correlation map (figure 3 (*d*)) showed that within a fracture domain, the successive sub-domains had the same orientation and also contained the same rectangular 2-D periodic lattice with parameters ($v = a\sqrt{2}$, $w = a\sqrt{3/2}$, $\gamma = 90°$) that were consistent with the ideal values of this crystallographic plane. Furthermore, these correlation maps showed that the sub-domains appeared as being (horizontally) shifted, one with respect to the others ($v/3 + w/2$). This apparent displacement could be easily related to the crystallographic relationship predicted between equivalent planes of the Q^{230} cubic structure taken perpendicularly to the [2 1 1] direction. As the [2 1 1] sub-domains were of large size, correlation averaging could be performed efficiently and led to the average motif shown in figure 3 (*b*).

The [1 1 0] fracture domains (figure 4) were rare and made of a complicated puzzle of small sub-domains displaying a lozenge-like striation. A thorough observation of these fracture domains revealed that the aspect of the sub-domains was not unique and that two kinds of periodic motifs, having the same cell parameters ($v = w = a\ (3/2)^{\frac{1}{2}}$, $\gamma = 109°28'$) could be observed. The low resolution of images of those distorted [1 1 0] fracture surfaces is revealed by the optical diffraction shown in figure 4 (*a*). As a consequence, the correlation averaging procedure was difficult to achieve in this case, but eventually yielded two distinct motifs [1 1 0]a and [1 1 0]b that are shown in figures 4 (*b*) and 4 (*c*). The Fourier filtered image shows an alternation of motifs between adjacent sub-domains and the presence of a relative (apparent) displacement between two successive (but non-adjacent) sub-domains of the same class that are fuly compatible with the symmetry of the *Ia*3*d* space group [22].

The cell parameter computed from the micrographs, $a = 8{\cdot}82 \pm 0{\cdot}13$ nm, is fully compatible with the values obtained by X-ray diffraction for the two related complexes ($a = 8{\cdot}4$ nm with $n = 9$ and $a = 11{\cdot}0$ nm with $n = 12$), especially if we take into account a frequently observed shrinking (≈5 to 10%) of the lattice due to freezing [22, 23].

4. Conclusion

One of the main conclusions which can be drawn from the above presented results is that it is possible to preserve the crystalline order of two and three dimensionally ordered high temperature thermotropic phases during the entire freeze-fracture replication process. When such preservation is achieved, image analysis of the micrographs (leading to the determination of the orientation of the different fracture planes, of their frequency and of the presence of symmetry elements) followed by the comparison with phases of known structure may be very useful for the structure determination of an unknown phase.

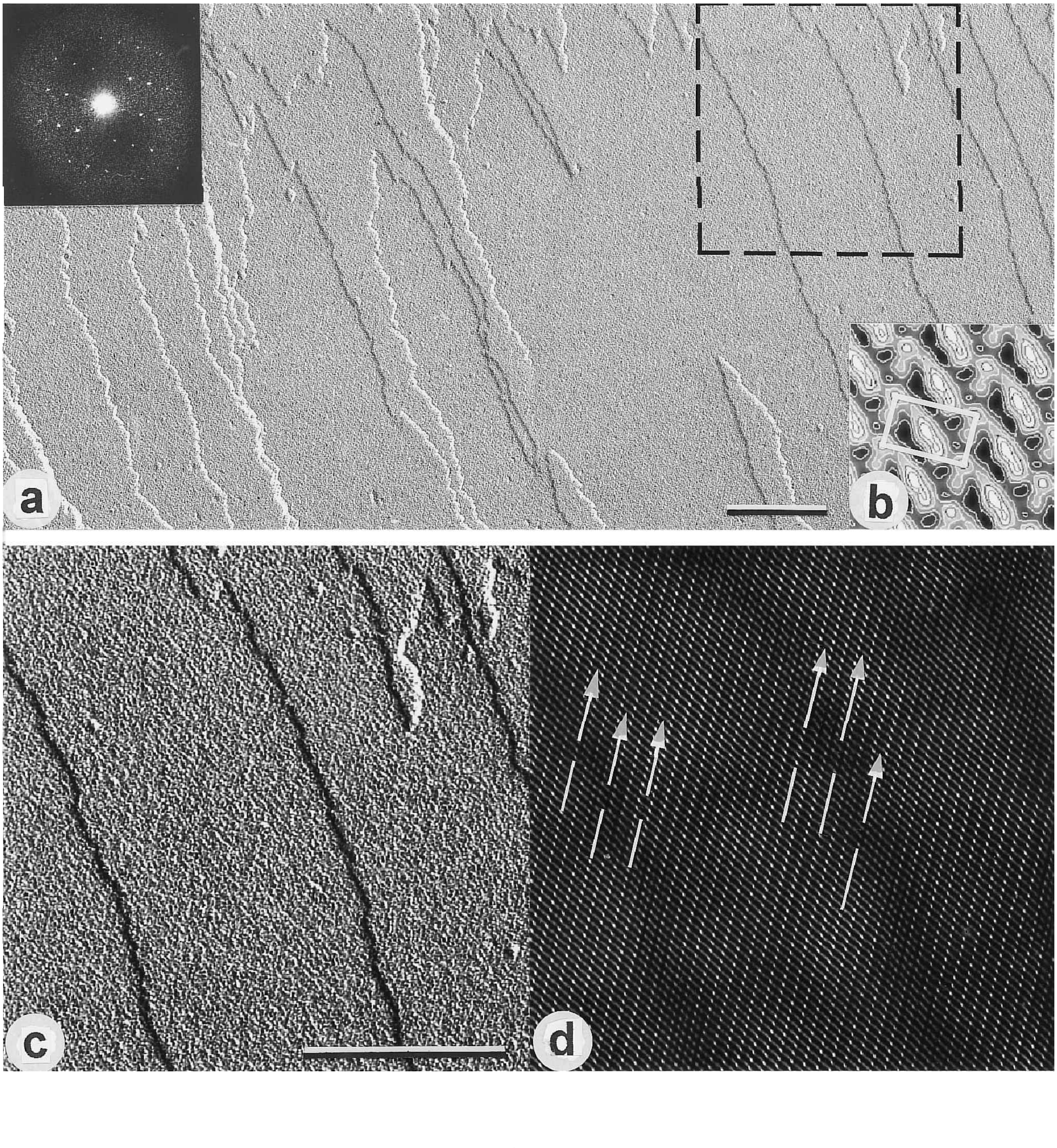

Figure 3. (*a*) Freeze-fracture electron micrograph of a [2 1 1] fracture domain for [Ag(11-,OPhVPy)$_2$][DOS] cubic phase. The optical diffraction of its central part is shown in the upper left corner and the CCR-averaged motif over almost 4000 elementary fragments in the bottom right corner (*b*). The apparent 2-D lattice parameters are: $v=a\sqrt{2}$, $w=a\sqrt{3/2}$ and $\gamma=90°$ with $a\approx 8{\cdot}95$ nm. An enlarged part of this electron micrograph, delimited by the dotted lines in (*a*), is shown in (*c*), and its cross correlation map, showing the shifts between successive subdomains (arrows), is shown in (*d*). The bars in (*a*) and (*c*) represent 200 nm.

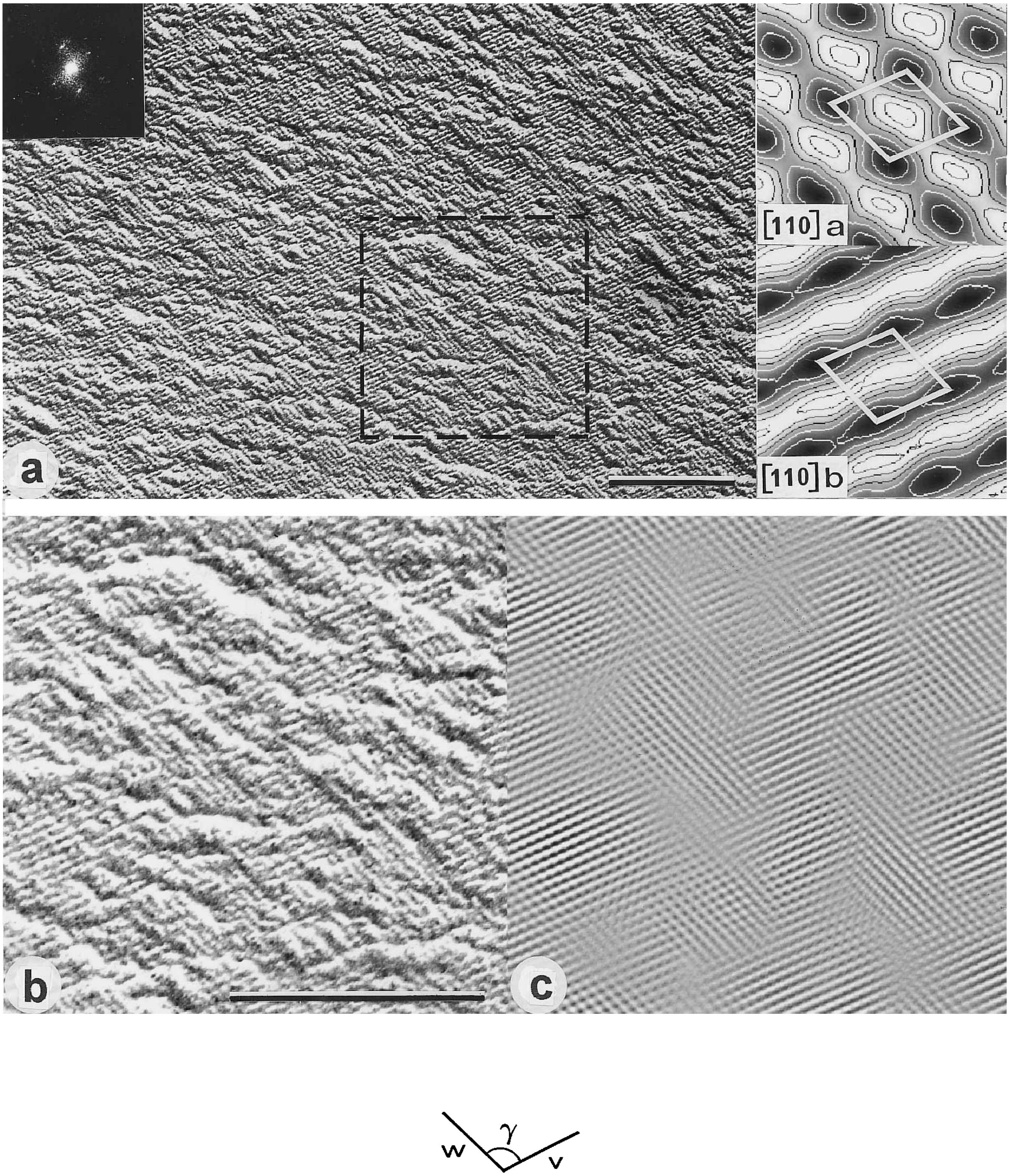

Figure 4. (*a*). Freeze-fracture electron micrography of a [1 1 0] fracture domain for [Ag(11-,OPhVPy)$_2$][DOS] cubic phase. The optical diffraction of its central part is shown in the upper left corner and the two CCR averaged motifs [1 1 0]a and [1 1 0]b corresponding to successive sub-domains are shown on the right part of the electron micrograph. The apparent 2-D lattice parameters are: $v=w=a\sqrt{3}/2$ and $\gamma=109°28'$ with $a\approx 8{\cdot}73\,\mathrm{nm}$. An enlarged part of this electron micrograph, delimited by the dotted lines in (*a*), is shown in (*b*). By Fourier filtering of (*b*), (*c*) shows the alternation of the two motifs [1 1 0]a and [1 1 0]b within a domain and also the relative displacement between two subdomains of the same class. The bars in (*a*) and (*b*) represent 200 nm.

References

[1] Fontell, K., 1981, *Mol. Cryst. Liq. Cryst.*, **63,** 59; Fontell, K., 1990, *Colloid Polym. Sci.*, **268,** 264.

[2] Luzzati, V., Tardieu, A., and Gulik-Krzywicki, T., 1968, *Nature*, **220,** 485; Mariani, P., Luzzati, V., and Delacroix, H., 1988, *J. mol. Biol.*, **204,** 165; Seddon, J. M., Hogan, J. L., Warrender, N. A., and Pebay-Peyrovla, E., 1990, *Progr. Colloid Polym. Sci.*, **81,** 189.

[3] Gray, G. W., and Winsor, P. A., 1974, *Mol. Cryst. liq. Cryst.*, **26,** 305.

[4] Seddon, J. M., and Templer, R. H., 1993, *Phil. Trans. R. Soc. Lond. A*, **344,** 377.

[5] Luzzati, V., and Spegt, P. A., 1967, *Nature*, **215,** 701.

[6] Anderson, S., Hyde, S. T., Larsson, K., and Lidin, S., 1988, *Chem. Rev.*, **88,** 221; Charvolin, J., 1990, *Contemp. Phys.*, **31,** 1; Charvolin, J., 1991, *Mol. Cryst. liq. Cryst.*, **198,** 145.

[7] Rançon, Y., and Charvolin, J., 1988, *J. phys. Chem.*, **92,** 2646; Clerc, M., Levelut, A. M., and Sadoc, J. F., 1991, *J. Phys. II Fr.*, **1,** 1263; Mariani, P., Amaral, L. Q., Saturni, L., and Delacroix, H., 1994, *ibid.*, **4,** 1393.

[8] (*a*) Gray, G. W., Jones, B., and Marson, F., 1957, *J. chem. Soc.*, 393; Kutsumizu, S., Yamada, M., and Yano, S., 1994, *Liq. Cryst.*, **16,** 1109; Etherington, G., Leadbetter, A. J., Wang, X. J., Gray, G. W., and Tajbakhsh, A., 1986, *Liq. Cryst.*, **1,** 209; (*b*) Demus, D., Gloza, A., Hartung, H., Hauser, A., Rapthel, I., and Wiegeleben, A., 1981, *Cryst. Res. Tech.*, **16,** 1445; (*c*) Kohne, B., Praefcke, K., and Billard, J., 1986, *Z. Naturforsch.*, **41b,** 1036; (*d*) Billard, J., Zimmermann, H., Pouko, R., and Luz, Z., 1989, *J. Phys. Fr.*, **50,** 539; (*e*) Fang, Y., Levelut, A. M., and Destrade, C., 1990, *Liq. Cryst.*, **7,** 265; (*f*) Levelut, A. M., and Fang, Y., 1990, *Coll. Phys.*, *C7*, **51,** 229; (*g*) Lattermann, G., and Staufer, G., 1990, *Mol. Cryst. liq. Cryst.*, **191**, 199; (*h*) Staufer, G., Schellhorn, M., and Lattermann, G., 1995, *Liq. Cryst.*, **18,** 519; (*i*) Weissflog, W., Pelzl, G., Letko, I., and Diele, S., 1995, *Mol. Cryst. liq. Cryst.*, **260,** 157; (*j*) Fischer, S., Fischer, H., Diele, S., Pelzl, G., Jankowski, K., Schmidt, R. R., and Vill, V., 1994, *Liq. Cryst.*, **17,** 855; (*k*) Stebani, U., Lattermann, G., Festag, R., Wittenberg, M., and Wendorff, J. H., 1995, *J. mater. Chem.*, **5,** 2247.

[9] Levelut, A. M., Germain, C., Keller, P., Liebert, L., and Billard, J., 1983, *J. Physique*, **44,** 623; Letko, I., Diele, S., Pelzl, G., and Weissflog, W., 1995, *Mol. Cryst. liq. Cryst.*, **260,** 171; Letko, I., Diele, S., Pelzl, G., and Weissflog, W., 1995, *Liq. Cryst.*, **19,** 643.

[10] Bruce, D. W., Dunmur, D. A., Hudson, S. A., Lalinde, E., Maitlis, P. M., McDonald, M. P., Orr, R., Styring, P., Cherodian, A. S., Richardson, R. M., Feijoo, J. L., and Ungar, G., 1991, *Mol. Cryst. liq. Cryst.*, **206,** 79.

[11] Adams, H., Bailey, N. A., Bruce, D. W., Davis, S. C., Dunmur, D. A., Hempstead, P. D., Hudson, S. A., and Thorpe, S., 1992, *J. mater. Chem.*, **2,** 395.

[12] Bruce, D. W., Donnio, B., and Fernihough, C., unpublished results.

[13] Bruce, D. W., unpublished results.

[14] Bruce, D. W., and Hudson, S. A., 1994, *J. mater. Chem.*, **4,** 479.

[15] Bruce, D. W., Donnio, B., Hudson, S. A., Levelut, A. M., Megtert, S., Petermann, D., and Veber, M., 1995, *J. Phys. II Fr.*, **5,** 289.

[16] Bruce, D. W., Donnio, B., Guillon, D., Heinrich, B., and Ibn-Elhaj, M., 1995, *Liq. Cryst.*, **19,** 537.

[17] Tardieu, A., and Billard, J., 1976, *J. Phys. Fr.*, *C3*, **37,** 79; Lydon, J. E., 1981, *Mol. Cryst. liq. Cryst. Lett.*, **72,** 79; Guillon, D., and Skoulios, A., 1987, *Europhys. Lett.*, **3,** 79.

[18] Gulik-Krzywicki, T., 1975, *Biochim. Biophys. Acta*, **415,** 1; Gulik-Krzywicki, T., and Costello, J., 1978, *J. Microsc.*, **112,** 103; Gulik-Krzywicki, T., Aggerbeck, L. P., and Larsson, K., 1984, *Surfactant in Solution*, edited by K. Mittal and B. Lindman (New York: Plenum Press), p. 237.

[19] Luzzati, V., Vargas, R., Gulik, A., Mariani, P., Seddon, J. M., and Rivas, E., 1992, *Biochemistry*, **31,** 279; Gulik, A., Delacroix, H., Kirschner, G., and Luzzati, V., 1995, *J. Phys. II Fr.*, **5,** 445.

[20] Delacroix, H., Gilli, J. M., Erk, I., and Mariani, P., 1992, *Phys. Rev. Lett.*, **69,** 2935; Dumoulin, H., Pieranski, P., Delacroix, H., Erk, I., Gilli, J. M., and Lansac, Y., 1995, *Mol. Cryst. liq. Cryst.*, **262,** 221.

[21] Ihn, K. J., Zasadzinski, J. A. N., Pindak, R., Slaney, A. J., and Goodby, J., 1992, *Science*, **258,** 275.

[22] Delacroix, H., Mariani, P., and Gulik-Krzywicki, T., 1990, *J. Phys. C. Fr.*, **51,** 119; Delacroix, H., Gulik-Krzywicki, T., Mariani, P., and Risler, J. L., 1993, *Liq. Cryst.*, **15,** 605.

[23] Delacroix, H., Gulik-Krzywicki, T., Mariani, P., and Luzzati, V., 1993, *J. Mol. Biol.*, **229,** 526; Gulik-Krzywicki, T., and Delacroix, H., 1994, *Biol. Cell.*, **80,** 193; Delacroix, H., Gulik-Krzywicki, T., and Seddon, J. M., 1996, *J. Mol. Biol.*, **258,** 88.

[24] Saxton, W. O., and Frank, J., 1977, *Ultramicroscopy*, **2,** 219; Frank, J., Goldfarb, W., Eisenberg, D., and Baker, T. S., 1978, *Ultramicroscopy*, **3,** 283.

[25] Q^n cubic phase of space group No. *n*, *International Tables for X-ray Crystallography*, 1952 (Birmingham: Kynoch Press).